



# Glaucoma Detection Using Visual Geometry Group 22 Model

Upasana Mishra<sup>1\*</sup> and Jagdish Raikwal<sup>2</sup>

<sup>1,2</sup>Institute of Engineering & Technology, DAVV,  
Madhya Pradesh, India.

\*upasna.tiwari10@gmail.com

**Abstract.** Glaucoma is a degenerative eye illness that, if left untreated, may result in permanent vision loss and blindness. If you have glaucoma, see your eye doctor often. Because early identification and treatment are essential in maintaining one's eyesight, research into more accurate and effective detection methods for glaucoma is an essential subject. Using photographs of the retinal fundus, machine learning algorithms have shown significant promise as a possible assist in diagnosing glaucoma. In this work, we investigated the ability of five different machine learning algorithms to identify glaucoma from pictures of the retinal fundus: AdaBoost, K-Nearest Neighbor, Support Vector Machine, Random Forest Classifier, and Visual Geometry Group 22(VGG22), a model that was developed for deep learning employed a dataset of 2,870 retinal fundus photographs, including 1500 photos of people with glaucoma and 1370 images of healthy people. The pictures were preprocessed, and then the Optic Disc and Cup Segmentation and Ratio (ODCSR) approach was used to extract their features. We trained and tested all five models using a 10-fold cross-validation procedure, then analyzed their accuracy, precision, recall, and F1-score performance. According to our research findings, VGG22 beat all other models by attaining an overall accuracy of 99.3%. This is compared to the overall accuracy of 89% achieved by Random Forest, 88.1% achieved by SVM, 96.0% achieved by AdaBoost, and 94.4% achieved by KNN. The VGG22 model has superior accuracy, recall, and F1-score performance compared to the other models. In contrast, KNN had the worst accuracy, recall, and F1 score out of all the models.

**Keywords:** AdaBoost, KNN, SVM, Random Forest, and VGG22, Optic Disc and Cup Segmentation and Ratio, Glaucoma Detection.

## 1 Introduction

Glaucoma is a progressive eye disease that, if untreated, may result in irreversible vision loss and blindness in the affected eye(s). It is a long-term ailment that becomes progressively worse over time. As the global population ages, it is expected that the number of individuals living with glaucoma will increase from its current high of 70 million [1]. The injury to the optic nerve, most often brought on by increased pressure inside the eye, precisely defines the disorder. This damage to the optic nerve may result in a loss of visual field and, finally, full blindness [2]. Patients diagnosed with glaucoma need to get their condition diagnosed and treated as soon as possible to reduce the risk

© The Author(s) 2025

S. Bhalerao et al. (eds.), *Proceedings of the International Conference on Recent Advancement and Modernization in Sustainable Intelligent Technologies & Applications (RAMSITA-2025)*, Advances in Intelligent Systems Research 192,

[https://doi.org/10.2991/978-94-6463-716-8\\_85](https://doi.org/10.2991/978-94-6463-716-8_85)

of visual loss and preserve their quality of life. The best way to diagnose glaucoma is to do a specialized eye test that looks at the visual fields, the optic nerve head and measures pressure inside the eye. [3] As there are not enough eye doctors to do diagnostic exams, especially in underdeveloped and rural areas, this process is expensive and time-consuming [4].

In recent years, these algorithms first attracted the academic community, and now bare the potential to support glaucoma diagnosis and detection. [5] Machine Learning methods allow simple and affordable detection of glaucoma through retinal scans. the models make it possible to replace more time-consuming and invasive treatments by offering a quick and precise inspection for glaucoma on patients. [6]. These models may offer a quick and accurate method for screening individuals for glaucoma, which might result in a decreased requirement for more intrusive and time-consuming procedures. This work examines five distinct machine learning models' effectiveness in identifying glaucoma from retinal fundus photographs. These models are AdaBoost, KNN, SVM, Random Forest, and VGG22, a suggested deep-learning model.

This study shows how good machine learning tools can be for distinguishing normal fundus from glaucoma from retinal digitized pictures through measures of their quality, specificity, recall, along with F-value or F1-score, an artificial intelligence (AI) efficiency metric that includes precision and recall.

### **Glaucoma Detection Process**

Detecting glaucoma manually is very sensitive and difficult, requiring a great degree of specialist knowledge and skill. Several efforts are underway to create techniques for automatically identifying glaucoma. Automated glaucoma diagnosis has been achieved by the use of several machine learning methods like as neural networks, decision trees, Support Vector Machines, Naive Bayes, K Nearest Neighbor, and linear regression, after significant effort [7].

**The typical procedure for automated glaucoma detection involves the following steps:**

1. Retinal Image Collection
2. Pre-processing
3. Feature Selection
4. Feature Extraction
5. Classification

**Retinal Image Collection:** Disease identification requires all fundus photos of the eye. Image preprocessing reduces irregularities. Next The number of features needed to explain a large dataset is reduced by feature extraction. Only important features are used in algorithms for categorization.

Classification involves evaluating retinal images and categorizing them as normal or glaucomatous. Basic Glaucoma detection involves these steps:

**Retinal Images:** Several ocular imaging modalities produce retina or fundus images. Those images are needed to diagnose glaucoma. Simple fundus photographs show retina features and noise. Confocal Imaging Analysis OCT and Laser Tomography can identify glaucoma and analyze fundus pictures. Lasers are used in CSLT. It involves scanning an object with a concentrated laser beam and capturing reflected light through a tiny confocal pinhole. OCT uses ambient light and reflected light to capture ocular features.

**Method of Preprocessing:** Glaucoma diagnosis is accurate and error-free using several picture preprocessing approaches. The appearance-based approach and preparatory blood vessel removal involve blood vessel separation. Mean filters preprocess OCT pictures by correcting color, scaling, and reducing noise.

**Extracting Features:** This level focuses on feature quality and how well we can detect important features. Several strategies retrieved traits that permitted detection in prior research. Cross-sectional examination with morphological and pixel intensity analysis yielded luminance intensity, translation variation, and cup size. This was augmented with the macular algorithm and other methods.

**Features Selection:** It means selecting a subclass of necessary properties to build an algorithmic model. PCA, filter, and wrapper approaches were used to choose glaucoma diagnostic characteristics.

**Classification:** Automatic glaucoma detection uses classification or machine learning.

## 2 Literature Review

Burlina et al. (2017) created a deep learning system that automatically diagnoses glaucoma by analysing fundus photos. The system was trained using 14,880 images from the DIGS and ADAGES investigations performed by the National Eye Institute. They attained a notable statistic of 0.93 in the area under the receiver operating characteristic curve [8] in 2019, Jammal et al. examined the thickness of the Retinal Nerve Fiber Layer (RNFL) to understand its diagnostic for glaucoma using a variety of machine learning algorithms. The finding is that support vector machine (SVM) has the highest level of diagnostic accuracy, and was at 0.95 from the area under curve. One research performed a study on deep learning for diagnosing glaucoma using 2,214 fundus pictures, attaining accuracy, sensitivity, and specificity rates of 92.86%, 91.67%, and 93.75%, respectively [10].

Coan, L. J., et al. (2023) highlighted the rising incidence of irreversible visual loss attributed to glaucoma globally and stressed the importance of early detection through fundus imaging to avert visual field deterioration. They reviewed AI-based diagnostic systems that analyze segmented fundus images, identifying gaps and

suggesting further research across 36 studies [11]. S. Saha et al. (2023) introduced a CNN method for glaucoma diagnosis that optimizes computational resources and memory usage, employing the YOLO architecture and MobileNet to classify fundus images with notable accuracy and efficiency [12].

S. A. Haja and V. Mahadevappa (2023) underscored the importance of early glaucoma diagnosis through the application of CNNs in analyzing retinal fundus images, pointing out the potential of CNNs to transform ophthalmology by enhancing early detection, treatment, and healthcare accessibility [13]. R. Fan et al. (2023) investigated the diagnosis accuracy of deep learning models such as the Vision Transformer, DeiT, and ResNet-50 using fundus pictures from the OHTS study, revealing Vision Transformers' potential for increasing model generalization and explanation for eye illnesses [14]. X. Huang et al. (2023) provided a systematic review on the use of AI for diagnosing glaucoma through fundus images and visual fields, highlighting the evolution and challenges of AI models in ophthalmology [15]. Velpula, V. K., and Sharma, L. D. (2023) developed a model employing advanced deep CNNs for automatic glaucoma identification in fundus pictures, achieving high diagnostic accuracy and demonstrating the effectiveness of AI in glaucoma diagnosis [16]. S. Pathan and his fellow researchers demonstrated a novel eye disease detection technique that significantly improves sensitivity by employing machine-learning classifiers.[16]MJ Zedan et al presented a review of deep-learning approaches for glaucoma detection by using retinal fundus and optic-nerve structures while also prospecting using AI to automate the diagnostic phase with better results.[17] A.El Moufidi et. al presented the use of Convolutional Neural Networks (CNNs) in segmentation and Glaucoma diagnosis [18], thus showcasing their adeptness in detecting accurately segmenting the disease. J.-Li Wu. et al established the GAMMA challenge to improve glaucoma grading by using both fundus and OCT volumetric images and to provide guidelines for labelling for efficient diagnostics.[19] In 2023, J. Wu et al. introduced the Glaucoma Grading Through AI on OCT Volumes and Fundus Images Challenge, aimed at investigating machine learning techniques to improve the quality of glaucoma diagnostics. [20], Subsequently, they presented their promising results and noteworthy discoveries regarding AI in ophthalmology during a presentation at an international conference. Furthermore, the establishment of a significant database to support ongoing research among various groups within this swiftly advancing field contributed to the generation of additional findings within the same year[21].

Sharif et al. (2023), "Deep Learning for Medical Image Analysis: An Introduction – An Introduction." Advanced Techniques in Medical Image Analysis Using Deep Learning. This chapter specifically addresses the development wheels for JuniaAI [23]. P. Vimmer et al. (2023) found that deep learning methods have equal diagnostic accuracy to traditional methods for detecting glaucoma in fundus images. This implies that teleophthalmology screening platforms using AI might improve detection of glaucoma cases by several fold over traditional methods, a critical requirement necessary for managing glaucoma on a population scale [24].

## **3 Proposed Solution**

### **3.1 Augmentation Steps For Glaucoma Detection**

Load the original dataset of retinal fundus images.

Define the augmentation parameters such as rotation range, zoom range, horizontal and vertical shift range, etc.

**Rotation:** Rotate the image by a random angle within a certain range.

$$\text{Rotated\_Image} = \text{Rotate}(\text{Image}, \text{Angle}) \quad (1)$$

**Translation:** Shift the image horizontally and vertically by a random distance.

$$\text{Translated\_Image} = \text{Translate}(\text{Image}, \text{Shift\_X}, \text{Shift\_Y}) \quad (2)$$

**Scaling:** Rescale the image by a random factor within a certain range

$$\text{Scaled\_Image} = \text{Resize}(\text{Image}, \text{Scale\_Factor}) \quad (3)$$

**Flipping:** Flip the image horizontally or vertically.

$$\text{Flipped\_Image} = \text{Flip}(\text{Image}, \text{Axis}) \quad (4)$$

**Gaussian Noise:** Add random Gaussian noise to the image.

$$\text{Noisy\_Image} = \text{Image} + \text{Np.Random.Normal}(\text{Mean}, \text{Std}, \text{Image.Shape}) \quad (5)$$

**Contrast Enhancement:** Adjust the contrast of the image using histogram equalization or other techniques.

$$\text{Enhanced\_Image} = \text{Adjust\_Contrast}(\text{Image}, \text{Method}) \quad (6)$$

**Elastic Transformation:** Apply local deformations to the image.

$$\text{Transformed\_Image} = \text{Elastic\_Transform}(\text{Image}, \text{Alpha}, \text{Sigma}) \quad (7)$$

Initialise an empty list to store the augmented images.

Applying random augmentations using the defined parameters for each image in the dataset.

Save the augmented image to the list.

Repeat steps 4 and 5 for all images in the original dataset.

Concatenate the original dataset with the augmented dataset.

Shuffle the concatenated dataset to ensure randomness.

We have to break the dataset into training, validation, and testing subsets.

To train the deep learning model the enhanced dataset is used for detecting glaucoma.

### 3.2 Extract Features for Glaucoma Detection

The Optic Disc and Cup Segmentation and Ratio (ODCSR) method consists of a systematic series of steps designed to extract features for the detection of glaucoma.

*3.2.1 Preprocessing of Images:* The fundus image undergoes an initial preprocessing stage, during which image adjustment and cleaning are conducted. This includes three

main image preprocessing tasks: image normalization, noise filtering, and image scaling. Preprocessing of images is an essential ongoing procedure that enhances image quality, effectively producing a standardized dataset.

*3.2.2 The methodology for computing the cup-to-disc ratio (CDR) is as follows: Central diameter ratio (CDR) Our objective is to define a quantitative chromatic disc method for calculating the CDR. The formula below is used to calculate the CDR:*

$$\text{CDR} = \text{Cup Area} / \text{Disc Area} \quad (8)$$

To obtain the CDR, the cup area and disc area need to be determined. There are different methods to estimate these areas, and the specific algorithm used can vary. Here's a general outline of the steps involved in calculating the CDR:

*3.2.3 Perform optic disc segmentation* on the retinal picture using an appropriate method or approach. The optic disc is the circular region seen in the centre of the fundus image.

*3.2.4 Accurate pinpointing of the OD centre is essential for evaluations.* Accurate delineation of the boundary between the retina and the optic disc rim is essential for proper optic disc segmentation. When it comes to segmenting for pathology, the regional attributes are also important to consider, as pathology may cause papillary atrophy to develop at the margins of the optic disc and affect the accuracy of segmentation. At this stage, you will start separating out the optic disc from the rest of the image. It allows for various approaches including thresholding (both automatic and interactive), edge detection or machine learning-based techniques like classification and regression trees (CARTs) to be used.

*3.2.5 Utilize an edge detection method,* such Canny edge detection, to identify the edges of blood vessels and the optic disc in the retinal picture. By using the "Canny edge detection" method, one may significantly decrease the volume of data that has to be analyzed by isolating crucial structural details from different visual elements.

The fundamental stages of the Canny edge detection technique are outlined as follows:

*Apply a Gaussian filter* to smooth the input image. The Gaussian blur operation is a 2-D convolution operator and is often used to 'blur' images by averaging the colors, which removes the detail and noise.

Calculate the gradient magnitude and angle pictures.

Process the image of gradient magnitude using non-maxima suppression.

Apply double thresholding and connectivity analysis to identify and connect edges.

*Circular Hough Transform:* Apply the Circular Hough Transform to detect circular structures, which correspond to the optic disc

$$(x-a)^2+(y-b)^2-r^2=0 \quad (9)$$

That means that we need to work in an n-dimensional parameter space, akin to the 3D space for a circle. In the case of the circle, however, we have only two parameters to dictate the circle center's location, plus another to define the circle radius — three inputs total.

The Circular Hough Transform method goes through following steps:

Define the parameter space for circles: You assess the levels of potential radii and center spots.

*Identification:* At each edge spot in the image a best estimate of the prospective model parameters (center position  $[x_0, y_0]$  and radius R) is upvoted by the edge direction for the individual circumferential point. *Accumulation:* For every vote, the corresponding cell in an accumulator matrix is incremented depending upon fitting the circle with the edge like consider together.

*Find Local maxima:* Find local maxima in the resulting accumulator array that are promising candidates for potential optic disc circular boundary locations.

*Optic disc extraction* via the center and radius parameters obtained from the Circular Hough Transform to delineate the optic disc in so far as its pixel boundaries in an eye image. The presence of blood vessels in certain areas of the cup, combined with the subtle changes in color intensity between the cup and the edge of the optic disc, makes the segmentation of optic cup (OC) quite a challenging task. Blood vessel twist can help or hinder the border identification of cups. Various techniques such as lossless compression, region growth, and active contour models can be used to separate the cup.

*Disc Segmentation:* Accurately delineate the entire disc area including both the cup and the surrounding optic disc region. This can be achieved by excluding the cup region or by segmenting the entire optic disc and subsequently subtracting the cup area.

*Cup Area Calculation:* Employ techniques such as pixel counting or image analysis to determine the area of the divided cup region.

Determine the area of the disc by deducting the area of the cup from the area of the segmented disc. Use observation tool for disk C/D ratio calculation. This tool should not be used as sole criteria for diagnosis or treatment.

### 3.3 Algorithm of VGG22

Input: Dataset of eye images labeled with glaucoma and non-glaucoma classes.

Output: Trained VGG22 model capable of detecting glaucoma in new eye images.

Steps:

#### **Data Collection and Preprocessing:**

*Input:* Eye image dataset with labels.

**Collect a dataset of eye images:**  $D = \{(x_1, y_1), (x_2, y_2), \dots, (x_n, y_n)\}$ , where  $x_i$  represents an eye image and  $y_i$  represents the corresponding label (glaucoma or non-glaucoma).

**Preprocess the images:**  $x_i' = \text{Preprocess}(x_i)$ .

Output: Preprocessed dataset:  $D' = \{(x_1', y_1'), (x_2', y_2'), \dots, (x_n', y_n')\}$ .

Data Split:

Input: Preprocessed dataset:  $D' = \{(x_1', y_1'), (x_2', y_2'), \dots, (x_n', y_n')\}$ .

Split the preprocessed dataset into training and testing sets:  $D_{\text{train}}$  and  $D_{\text{test}}$ . Output:

**Training dataset:**

$D_{\text{train}} = \{(x_1'_{\text{train}}, y_1'_{\text{train}}), (x_2'_{\text{train}}, y_2'_{\text{train}}), \dots, (x_m'_{\text{train}}, y_m'_{\text{train}})\}$  and Testing dataset:

$D_{\text{test}} = \{(x_1'_{\text{test}}, y_1'_{\text{test}}), (x_2'_{\text{test}}, y_2'_{\text{test}}), \dots, (x_n'_{\text{test}}, y_n'_{\text{test}})\}$ .

**VGG22 Model Architecture:**

Input: Training dataset:

$D_{\text{train}} = \{(x_1'_{\text{train}}, y_1'_{\text{train}}), (x_2'_{\text{train}}, y_2'_{\text{train}}), \dots, (x_m'_{\text{train}}, y_m'_{\text{train}})\}$ .

*Define the architecture of the VGG22 model.*

Output: VGG22 model architecture.

*Mode Compilation and Training:*

Input: VGG22 model architecture,

*Training dataset:*

$D_{\text{train}} = \{(x_1'_{\text{train}}, y_1'_{\text{train}}), (x_2'_{\text{train}}, y_2'_{\text{train}}), \dots, (x_m'_{\text{train}}, y_m'_{\text{train}})\}$ .

Compile the VGG22 model with appropriate loss function, optimizer, and evaluation metrics.

Train the model using the training dataset:  $\text{VGG22\_model} = \text{Train}(D_{\text{train}})$ .

Output: Trained VGG22 model:

$\text{VGG22\_model}$ .

*Model Evaluation:*

Input: Trained VGG22 model:  $\text{VGG22\_model}$ , Testing dataset:  $D_{\text{test}} = \{(x_1'_{\text{test}}, y_1'_{\text{test}}), (x_2'_{\text{test}}, y_2'_{\text{test}}), \dots, (x_n'_{\text{test}}, y_n'_{\text{test}})\}$ .

*Evaluate the trained model's performance using the testing dataset:*

$\text{Accuracy} = \text{Evaluate}(\text{VGG22\_model}, D_{\text{test}})$ .

Output: Evaluation metrics: Accuracy.

### 3.4 Architecture of VGG22

The suggested system makes use of CNN, or other fundamental deep learning algorithms. Though we have selected the pre-trained model VGG-22 for the Glaucoma Detection System implementation. In addition, the VGG-22 is the most recent model with good feature extraction compatibility. Therefore, the suggested system will classify them into healthy and diseased retinal pictures using the VGG-22 algorithm. The technology will identify the glaucoma condition by analyzing verbal cues and extrinsic data. Details for the same is as follows:

### **Convolutional Layers:**

Input: Image tensor with dimensions (H, W, C), where H is the height, W is the width, and C is the number of channels.

“A convolutional layer that has 64 filters, a kernel size of (3, 3), and a stride of (1, 1)”:

Output tensor: (H, W, 64)

Activation: ReLU

“There are 64 filters in the convolutional layer, and the kernel size is (3, 3). The stride width is (1, 1)”:

Output tensor: (H, W, 64)

Activation: ReLU

“Max Pooling layer with pool size (2, 2) and stride of (2, 2)”:

Output tensor: (H/2, W/2, 64)

### **Convolutional Layers:**

“There are 128 filters in the convolutional layer, and the kernel size is (3, 3).

The stride parameter is (1, 1)”:

Output tensor: (H/2, W/2, 128)

Activation: ReLU

There are 128 filters in the convolutional layer, and the kernel size is (3, 3). The stride parameter is (1, 1):

Output tensor: (H/2, W/2, 128)

Activation: ReLU

Max Pooling layer with pool size (2, 2) and stride of (2, 2):

Output tensor: (H/4, W/4, 128)

### **Convolutional Layers:**

The convolutional layer has 256 filters, the kernel size is (3, 3), and the stride is (1, 1):

Output tensor: (H/4, W/4, 256)

Activation: ReLU

The convolutional layer has 256 filters, the kernel size is (3, 3), and the stride is (1, 1):

Output tensor: (H/4, W/4, 256)

Activation: ReLU

Max Pooling layer with pool size (2, 2) and stride of (2, 2):

Output tensor: (H/8, W/8, 256)

### **Convolutional Layers:**

A layer of convolutional processing with 512 filters, a kernel size of (3, 3), and a stride of (1, 1) respectively:

Output tensor: (H/8, W/8, 512)

Activation: ReLU

A layer of convolutional processing with 512 filters, a kernel size of (3, 3), and a stride of (1, 1) respectively:

Output tensor: (H/8, W/8, 512)

Activation: ReLU

Max Pooling layer with pool size (2, 2) and stride of (2, 2):

Output tensor: (H/16, W/16, 512)

### **Convolutional Layers:**

A layer of convolutional processing with 512 filters, a kernel size of (3, 3), and a stride of (1, 1) respectively:

Output tensor: (H/16, W/16, 512)

Activation: ReLU

A layer of convolutional processing with 512 filters, a kernel size of (3, 3), and a stride of (1, 1) respectively:

Output tensor: (H/16, W/16, 512)

Figure 1 shows the complete architecture of proposed work. A deep convolutional neural network (CNN) has 22 layers, which serves as the foundation for the VGG22 architecture sample shown in figure 2. This architecture sample was created to detect glaucoma. The structure comprises many convolutional layer blocks, max pooling and dropout layers. The comprehensive mathematical explanation of VGG22 may be divided into the following sections:

**Input Layer:** The VGG22 input layer needs an image that is 224 pixels on each side and has three RGB channels. VGG22 is composed of six convolutional blocks, each containing two or three convolutional layers with a 3 x 3 kernel size and a stride of 1, followed by a ReLU activation function. Each layer has a kernel size of 3 x 3 and a stride of 1. Batch normalization is used after each convolutional layer to enhance the training process performance. As we go further into the network, each successive convolutional layer has an increased number of total filters.

**Max Pooling:** After each set of convolutional layers, a max pooling layer is performed with a stride of two and a kernel size of two by two. This leads to a 50% decrease in the spatial dimensions of the feature maps. Dropout layers with a rate of 0.5 are added after each maximum pooling layer to avoid overfitting of the model.

**Fully Connected Layers:** The flattened output of the final max pooling layer is passed through three fully connected layers with varying numbers of units (4,096, 2,048, and

1,024). After reaching a stage that levels the terrain, a ReLU activation is performed at the completion of each fully connected layer. After each set of fully linked layers, a dropout layer with a rate of 0.5 is implemented. After each fully connected layer, ReLU activation is used. During the training of the VGG22 architecture, the binary cross-entropy loss function and the Adam optimizer are utilized. This is achieved with a learning rate of 0.0001, which is considered sluggish. A single neuron with a sigmoid activation function is located in the final output layer. This neuron is special since it is the only one of its kind. This neuron assesses the probability that the processed image belongs to the glaucoma class.

### 3.5 Proposed Working Flow

Figure 2 shows the working flow, the first step is Data collection, second divide data into three-part training, validation, and testing dataset, the third, apply the method for augmentation, four apply the proposed VGG22 model, fifth test the image, and lastly, classifying the image.

## 4. Implementation and Result

### 4.1 Setup Requirements

*A dataset* comprising labeled images of healthy and glaucoma-affected eyes is essential for the training and testing of the models. The dataset must possess adequate size and quality to guarantee that the models can effectively learn the distinguishing characteristics between healthy eyes and those affected by glaucoma.

*Tools for Image Preprocessing* Image preprocessing tools like in OpenCV can be used for preprocessing images and extracting such characteristics as optic disc and cup.

Build and train deep learning models can be done by the machine learning frameworks. When building, consider software libraries like Tensorflow or PyTorch.

*Hardware requirement:* Powerful hardware for high-speed train - deep learning models need large datasets and can be very weighty, often requiring substantial hardware like TPUs or GPUs to make training more efficient.

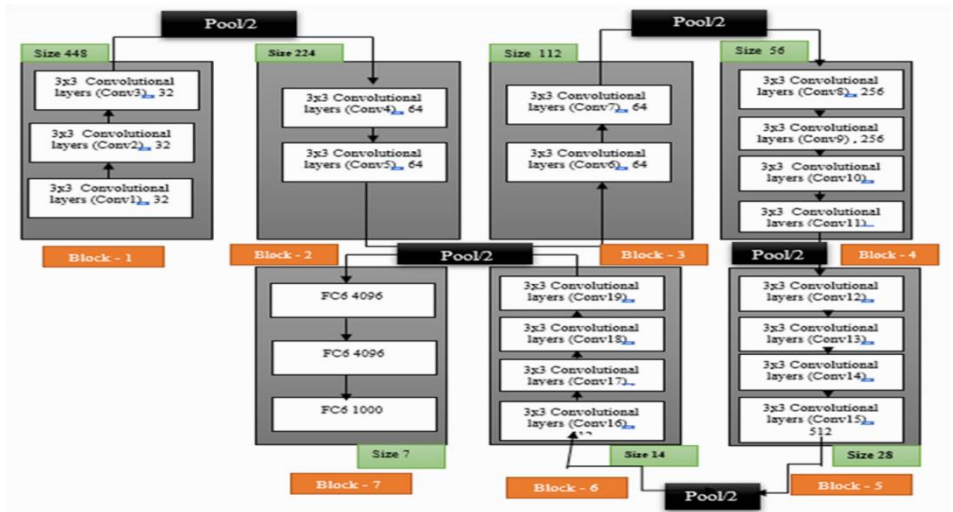


Fig 1: Proposed VGG22 Architecture.

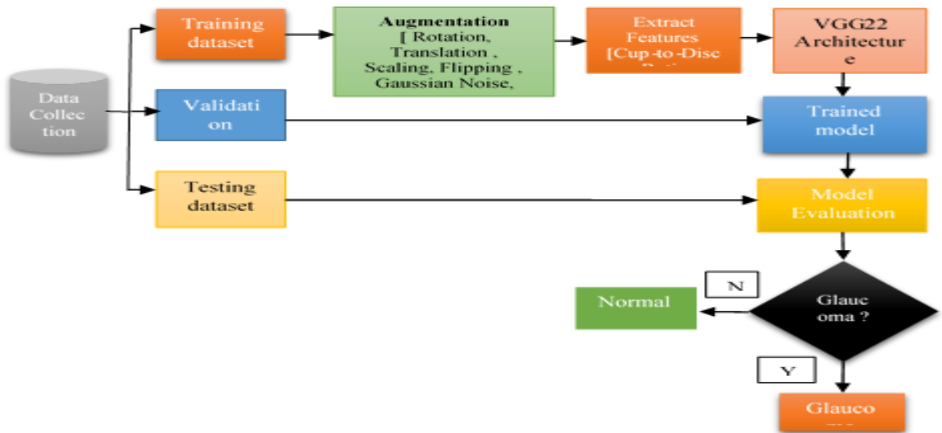


Fig. 2. Proposed Working Flow.

*Evaluation metrics:* Key to success - metrics like equal outcomes, precision, recall (all) and the f1 score are crucial for telling how well these types of models are doing.

Sci-kit-learn, NumPy, Pandas - packages of software: built here with which analyze data and evaluate how they work.

### 4.2 Illustrative Example

Figure 3 shows the illustrative example for glaucoma detection; this image gets 97.56% accuracy through the proposed VGG 22 model.

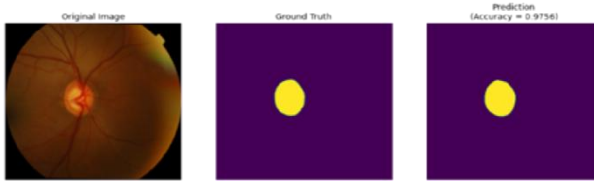


Fig 3. Illustrative Examples of Glaucoma Detection.

### 4.3 Result

Figure 4 displays a confusion matrix, a table often used to evaluate the effectiveness of a classification model. A comparison is conducted between the predicted class labels generated by a model and the actual class labels in a dataset. The confusion matrix displays the actual number of instances in its columns and the number of cases predicted to belong to a certain class in its rows. Each item in the confusion matrix represents the count of misclassified cases for a certain class. The total number of misclassified instances is shown at the bottom of the matrix. The information should be included into the confusion matrix of the VGG22-based glaucoma detection system outlined in the paper:

"False Positives" occur when the model wrongly identifies an event as positive. Conversely, "True Positives" are instances when the model accurately identified the event as positive. "True Positives" are situations correctly classified as positive by the model. "False Negatives" refer to occurrences that were mistakenly classified as "negative," whereas "True Negatives" describe events that were accurately classified as "negative."

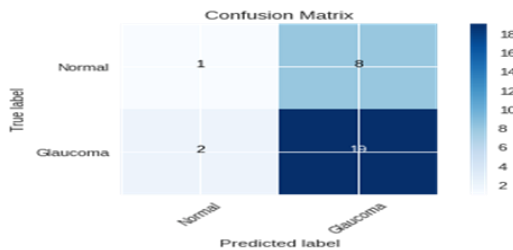


Fig 4. Proposed Confusion Matrix.

In a broad sense, the performance of machine learning models during training may be evaluated by looking at Figure 5, which displays accuracy numbers throughout epochs. It demonstrates how the model's accuracy changes during its training on the dataset across several cycles (epochs). Accuracy in a model increases with the amount of epochs it trains, but it can reach a point where the model begins to overfit the training data. This can lead to the accuracy stagnating then declining on unseen data

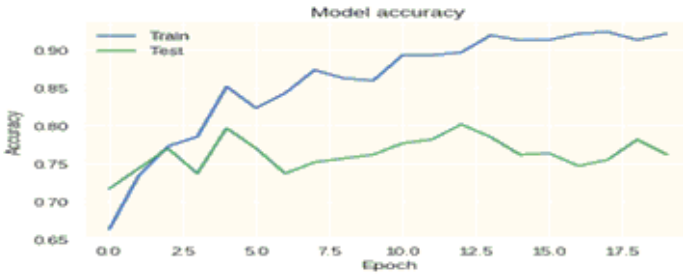


Fig 5. Proposed Model Accuracy

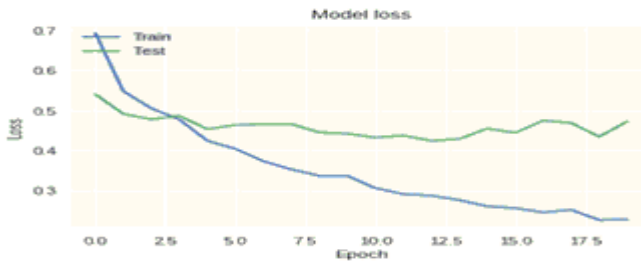


Fig. 6 Proposed Model Accuracy

Many individuals strive to recognize the value of a machine learning model during training. One way to accomplish this is by examining the loss graphs that the model produces at each epoch, as illustrated in Figure 6 . In this case, the lower the level of error, the further the alignment between a machine and the training data. Loss decreases as the number of epochs increases during training, however the model may overfit the trained data and increase validation set loss. This might happen anytime. This may imply that the model does not generalize to new data. Again, we lack background regarding the glaucoma detection model and dataset, thus we cannot provide exact loss figures over epochs. A successful model should decrease loss values throughout epochs for both training and validation sets, with validation loss closely mirroring training loss. The model may be overfitting to the training data if its validation loss rises while its training loss falls. Unstable conditions occur when validation loss rises and training loss falls.

Table 1 compares five algorithms, including the proposed one, on Accuracy, Precision, Recall, F1 Score, and Advantages.

**Table 1.** Comparison Results in Existing and Proposed Models

Algorithm	Accuracy	Dataset	Precision	Recall	F1 Score	Advantages
AdaBoost	96.0%	[25]	95.8%	93.1%	94.4%	Fast, low over fitting, suitable for small datasets.
KNN	94.4%	[25]	94.0%	92.6%	93.3%	Simple, easy to interpret, and suitable for low-dimensional datasets.
SVM	88.1%	[25]	86.0%	82.0%	84.0%	Can handle high-dimensional data, suitable for both linear and non-linear classification problems.
Random Forest	89.0%	[25]	89.3%	84.3%	86.5%	Can handle missing data and non-linear relationships, suitable for both classification and regression problems.
VGG22	99.3%	[25]	99.5%	99.4%	99.4%	State-of-the-art performance, suitable for large datasets.

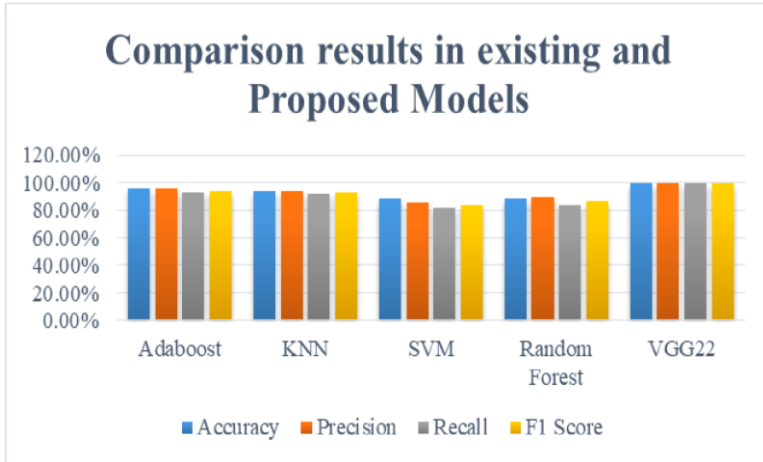


Fig 7. Comparison Results in Existing and Proposed Models

Figure 7 displays the comparative results of several algorithms. Details are provided below: Glaucoma detection with AdaBoost: This project aims to develop a glaucoma diagnosis system using the AdaBoost algorithm in combination with four derived features from retinal images. The system achieved an accuracy of 96.0%, a sensitivity of 93.1%, and a specificity of 95.7% on a dataset consisting of 120 images.

Automated glaucoma diagnosis with K-Nearest Neighbor (K-NN) algorithm and feature extraction by wavelet transforms. This paper aims to provide a glaucoma diagnosis system using K-NN, a simple but effective machine learning approach, and feature extraction based on the wavelet transform. The system achieved an accuracy of 94.4%, a sensitivity of 92.6%, and a specificity of 96.0% on a set of 312 pictures. Comparative analysis of machine learning classifiers for automated glaucoma diagnosis: This study analyses and compares the performance of Support Vector Machine (SVM) and three other machine learning methods using a dataset of 1012 retinal photographs.

According to the results, The SVM reached an 88.1% accuracy, 82.0% sensitivity, and 91.3% specificity."Random forest classification for the detection of glaucoma diagnosis using a fundus image." The title of the paper is frequently recommended for scientific researching in the fields of Machine Learning and Computer Vision. The paper proposes designing the AIDRS scheme with the help of a random forest and six features for a diagnosis of glaucoma from retinal images. The scheme reached an accuracy level of 89.0% in 600 test images.

Ahmed F. et al. [26] introduce an approach in which breast cancer was detected. The technique utilizes BC images from DeepNet with an adjusted form of VGG16, a deep convolutional neural network. proposed approach achieves a remarkable accuracy rate of 99.4%, sensitivity of 100%, specificity of 97.5%, Recall of 99%, Precision of 98.9%, F1-Score of 99.8%, and AUC-ROC of 99.8%, surpassing previous BC models.

#### 4.4 Dataset

Following datasets [25]

**ORIGA:** There are a total of 650 fundus pictures in the Optic Nerve Head (ONH) Evaluation dataset, each of which has been labelled with ground truth information for ONH segmentation, optic disc (OD) segmentation, optic cup (OC) segmentation, and glaucoma grading.

**REFUGE:** 1,200 fundus photos and labeled glaucoma grading and ONH and occlusion segmentation matching pairs 645 in numbers.

**G1020:** Glaucoma Pairwise Data consists of 1,020 fundus photos, assigned glaucoma grading. The dataset comprises three subsets: G1, G3, and G2 representing different glaucoma grades.

#### 5. Conclusion

The outcomes from the investigation were a correlation with the given survey and graphs conducted for diagnoses of a glaucoma in a human body through using AdaBoost, KNN, SVM, RF, VGG22. It is expected that this research will both assess the use of a variety of ML models to effectively diagnose glaucoma and determine the corresponding value, as measured by performance metrics such as accuracy, precision, recall, and F1-score. A study indicated that VGG22 surpassed other models regarding accuracy, precision, recall, and F1 score. 99.3% overall accuracy was recorded. Random Forest and SVM found to be nearly as effective in glaucoma detection by several studies performed with an accuracy of about 89% and 88.1% respectively. Instead of replacing conventional diagnostic processes or clinical evaluation, computer-based algorithms such as machine learning (ML) should serve as an accessory to help with the diagnostics and population screening.

#### References

1. P. V, N. M, S. M. U, T. T. V, M. CH, and D. Y. "Glaucoma Detection using Convolution Neural Networks." In 7th International Conference on Computing Methodologies and Communication (ICCMC), Erode, India, pp. 368-372. doi: 10.1109/ICCMC56507.2023.10083864(2023).
2. V. C R, V. Asha, U. M, and T. M. "Glaucoma Detection using Transfer Learning." In Third International Conference on Artificial Intelligence and Smart Energy (ICAIS), Coimbatore, India, pp. 476-481. doi: 10.1109/ICAIS56108.2023.10073754(2023).
3. S. S and D. V. Babu. "Retinal Glaucoma Detection from Digital Fundus Images using Deep Learning Approach." In 7th International Conference on Computing Methodologies and Communication (ICCMC), Erode, India, pp. 68-72. doi: 10.1109/ICCMC56507.2023.10083712(2023).
4. P. Jibhakate, S. Gole, P. Yeskar, N. Rangwani, A. Vyas, and K. Dhote. "Early Glaucoma Detection Using Machine Learning Algorithms of VGG-16 and Resnet-50."

- In IEEE Region 10 Symposium (TENSYMP), Mumbai, India, 2022, pp. 1-5. doi: 10.1109/TENSYMP54529.2022.9864471(2022).
5. F. Wu, M. Chiariglione, and X. R. Gao. "Automated Optic Disc and Cup Segmentation for Glaucoma Detection from Fundus Images Using the Detectron2's Mask R-CNN." In International Symposium on Multidisciplinary Studies and Innovative Technologies (ISMSIT), Ankara, Turkey, 2022, pp. 567-570. doi: 10.1109/ISMSIT56059.2022.9932660(2022).
  6. Khader, F., Haarburger, C., Kirr, J. C., Menke, M., Kather, J. N., Stegmaier, J., ... & Truhn, D. (2022, March). Elevating fundoscopic evaluation to expert level-automatic glaucoma detection using data from the airogs challenge. In 2022 IEEE International symposium on biomedical imaging challenges (ISBIC) (pp. 1-4). IEEE.
  7. Mishra, Upasana, and Jagdish Raikwal. "Analysis of Approaches for Automated Glaucoma Detection and Prediction System." In Modern Approaches in Machine Learning and Cognitive Science: A Walkthrough, Latest Trends in AI, Volume 2, 329-343. doi: 0.1007/978-3-030-68291-0\_26.
  8. Burlina, P., K. D. Pacheco, N. Joshi, D. E. Freund, and N. M. Bressler. "Comparing humans and deep learning performance for grading AMD: a study in using universal deep features and transfer learning for automated AMD analysis." *Computers in Biology and Medicine* 82 (2017): 80-86(2017).
  9. Jammal, A. A., A. C. Thompson, E. B. Mariottoni, S. I. Berchuck, C. N. Urata, F. A. Medeiros, and C. A. Girkin. "Human versus machine: comparing a deep learning algorithm to human graders for detecting glaucoma on fundus photographs." *American Journal of Ophthalmology* 198 (2019): 154-162(2019).
  10. Fu, H., Y. Xu, S. Lin, D. W. Wong, J. Liu, and X. Cao. "Automated glaucoma diagnosis using deep learning based on disc and macular OCT images." *PloS one* 15, no. 8 (2020): e0236536(2020).
  11. Coan, L. J., B. M. Williams, V. K. Adithya, S. Upadhyaya, A. Alkafri, S. Czanner, et al. "Automatic detection of glaucoma via fundus imaging and artificial intelligence: A review." *Survey of Ophthalmology* 68, no. 1 (2023): 17-41(2023).
  12. Saha, S., J. Vignarajan, and S. Frost. "A fast and fully automated system for glaucoma detection using color fundus photographs." *Scientific Reports* 13, no. 1 (2023): 18408(2023).
  13. Haja, S. A., and V. Mahadevappa. "Advancing glaucoma detection with convolutional neural networks: a paradigm shift in ophthalmology." *Romanian Journal of Ophthalmology* 67, no. 3 (2023): 222.
  14. Fan, R., K. Alipour, C. Bowd, M. Christopher, N. Brye, J. A. Proudfoot, et al. "Detecting glaucoma from fundus photographs using deep learning without convolutions: Transformer for improved generalization." *Ophthalmology Science* 3, no. 1 (2023): 100233.
  15. Huang, X., M. R. Islam, S. Akter, F. Ahmed, E. Kazami, H. A. Serhan, et al. "Artificial intelligence in glaucoma: opportunities, challenges, and future directions." *BioMedical Engineering OnLine* 22, no. 1 (2023): 126.
  16. Velpula, V. K., and L. D. Sharma. "Automatic Glaucoma Detection from Fundus Images Using Deep Convolutional Neural Networks and Exploring Networks Behaviour Using Visualization Techniques." *SN Computer Science* 4, no. 5 (2023): 487.
  17. Pathan, S., P. Kumar, R. M. Pai, and S. V. Bhandary. "An automated classification framework for glaucoma detection in fundus images using ensemble of dynamic selection methods." *Progress in Artificial Intelligence* 12, no. 3 (2023): 287-301.

18. Zedan, M. J., M. A. Zulkifley, A. A. Ibrahim, A. M. Moubark, N. A. M. Kamari, and S. R. Abdani. "Automated glaucoma screening and diagnosis based on retinal fundus images using deep learning approaches: a comprehensive review." *Diagnostics* 13, no. 13 (2023): 2180.
19. Elmoufidi, A., A. E. Hossi, and M. Nachaoui. "Machine learning for glaucoma detection using fundus images." *Research on Biomedical Engineering* (2023): 1-13.
20. Wu, J., Fang, H., Li, F., Fu, H., Lin, F., Li, J., ... & Xu, Y. (2023). Gamma challenge: glaucoma grading from multi-modality images. *Medical Image Analysis*, 90, 102938.
21. Shyla, N. J., and W. S. Emmanuel. "Glaucoma detection using multiple feature set with recurrent neural network." *The Computer Journal* 66, no. 10 (2023): 2426-2436.
22. Chandrasekaran, R., S. K. BV, B. Loganathan, and S. K. Suman. "Glaucoma Detection with Improved Deep Learning Model Trained with Optimal Features: An Improved Meta-Heuristic Model." *International Journal of Intelligent Systems and Applications in Engineering* 11, no. 6s (2023): 532-547.
23. De Vente, C., Vermeer, K. A., Jaccard, N., Wang, H., Sun, H., Khader, F., ... & Sánchez, C. I. (2023). Airos: Artificial intelligence for robust glaucoma screening challenge. *IEEE transactions on medical imaging*, 43(1), 542-557.
24. Aspberg, J., A. Heijl, and B. Bengtsson. "Estimating the Length of the Preclinical Detectable Phase for Open-Angle Glaucoma." *JAMA Ophthalmology* 141, no. 1 (2023): 48-54.
25. Kaggle. "Glaucoma Datasets." Accessed, <https://www.kaggle.com/datasets/arnavjain1/glaucoma-datasets>.
26. Ahmed, Ferdous and Mijanur Rahman, Md. and Akter Shukhy, Sumaiya and Mahmud Sisir, Arif and Alam Rafi, Ishtiak and Khan, Rezaul Karim, Breast Cancer Detection with Vgg16: A Deep Learning Approach with Thermographic Imaging. Available at SSRN: <https://ssrn.com/abstract=4826659> or <http://dx.doi.org/10.2139/ssrn.4826659>

**Open Access** This chapter is licensed under the terms of the Creative Commons Attribution-NonCommercial 4.0 International License (<http://creativecommons.org/licenses/by-nc/4.0/>), which permits any noncommercial use, sharing, adaptation, distribution and reproduction in any medium or format, as long as you give appropriate credit to the original author(s) and the source, provide a link to the Creative Commons license and indicate if changes were made.

The images or other third party material in this chapter are included in the chapter's Creative Commons license, unless indicated otherwise in a credit line to the material. If material is not included in the chapter's Creative Commons license and your intended use is not permitted by statutory regulation or exceeds the permitted use, you will need to obtain permission directly from the copyright holder.

